Analysis and Modeling of the LTE Broadband Channel for Train-Ground Communications on High-Speed Railway

Zhao Min*, Wu Muqing*, Sun Yanzhi*, Jia Guiyuan*
Di Shiping†, Zhou Panfeng†, Zeng Xiangbing†, Ge Shuyun†
*Laboratory of Network System Architecture and Convergence
Beijing University of Posts and Telecommunications, Beijing 100876, China
†Design Section of Communication, CRSCD, Bejing 100073, China

***Abstract*—The increasing interest that has been drawn to LTE system used in High-Speed Railway therefore requires measurement and analysis of broadband mobile channel for train-ground communications. By the approval of the Ministry of Railways of China, extensive and practical measurements are performed on Harbin-Dalian passenger dedicated line with the maximum running speed of 370 km/h. Based on the hierarchical two-hop network structure, this paper first presents comprehensive analyzed results of channel characteristics in viaduct scenario, including both the large-scale and small-scale fading parameters. The proposed path loss model benefits LTE system link budget and feasible transceiver-range determination. In particular, channel impulse response, power delay profile, the delay spread, the number of paths and delay-Doppler spectrum are extracted, evaluated and reported. All these informative results promote the evaluation and verification of broadband communication system on High-Speed Railway.**

I. Introduction

High-Speed Railway (HSR), as a rapid, convenient and green public transportation system, has recently made great progress and attracted increasing amount of attention. Trains with a speed of more than 300 km/h have been developed rapidly all over the world. In contrast with the great progress of HSR, there is still a huge gap between the existing low-rate services and the demand for larger capacity and higher quality of the communication system for HSR [1]. Long term evolution (LTE), due to its low latency, high data-transfer rate, low cost and IP-based network, has great advantages in high-speed scenarios. It is commonly deemed to be the next generation of wireless communication system for HSR. LTE can provide reliable and efficient wireless services for both railway-specific signaling, and communications by passengers.

For HSR wireless communications system design and evaluation, two main aspects are required: a) an accurate model for path loss (PL) and shadow fading (SF), and b) descriptions of rapid undulation of channel characteristics over a short period of time or distance. Some measurements and models for HSR have been performed and reported. Table I gives a brief review and classification of them.

For engineering implementations, HSR environments consist of different scenarios which are distinct from standard suburban and rural environments in cellular communications. These new scenarios put forward new challenges. So the narrowband researches on channel properties in viaduct [1], cutting [2] and tunnel [3] scenarios have been done at 930 MHz for GSM systems [4]. Taking different center frequency, bandwidth and mobility of the system into account, they affect the channel characteristics such as the PL, frequency selectivity and Doppler behavior. Therefore, the specifics of broadband channels were reported in [5-8]. Only in [7], the train-ground communication system has been studied. For safety reasons and geographical limitations, in [7], the antenna height was quite low and the distance between the BS and the track was larger than that in practical case. Since its measurement setup did not fully match the practical HSR scenario or D2a reference setup in [6], all these affect the results of research. Therefore, a reliable investigation of the HSR channel for LTE system is urgently needed.

The main contribution of our works is performed practical HSR propagation measurements by the approval of the Ministry of Railways of China. Under the hierarchical two-hop network structure, the train CRH380B was used exclusively for measurement purposes and the transmit (Tx) antenna was mounted on the signal tower also by approval. Using a LTE sounding signal with 20 MHz bandwidth at 2.6 GHz for slippage correlation algorithm, the collected data are processed for large-scale and small-scale channel characteristics, such as channel impulse response (CIR), power delay profile (PDP), the number of paths, delay spread (DS) and Doppler spectrum. In particular, PL exponent and SF parameter are evaluated to derive the empirical log-distance PL model. The rest of the paper is organized as follows. Section II states the network structure for HSR succinctly. Measurement environment, equipments, and procedures are reported in Section III. In Section IV, measured data are analyzed to extract large-scale parameters and derive PL model. In Section V, small-scale characteristics results are shown and discussed. Finally, conclusions are drawn in Section VI.

II. Network Structure

A reasonable network structure is the basis of a communication system. When conventional cellular systems are deployed

978-1-4673-6187-3/13/$31.00 ©2013 IEEE

TABLE I
CHANNEL MEASUREMENTS ON HSR

Measurement	Carrier frequency	Frequency-selectivity	Environments	Channel statistics
[1]	930 MHz	narrowband	viaduct scenario in ZX HSR	LCR, AFD, PL, SF, K-factor
[2],[3]	930 MHz	narrowband	cutting and plain scenario in ZX HSR	PL, SF, K-factor, DS
[4]	930 MHz	narrowband	WG HSR	PL, SF, K-factor, DS
[5]	2.1 GHz	broadband	viaduct scenario in ZX HSR	PL, SF, K-factor, DS
[6]	5 GHz	broadband	in Germany,between Siegburg and Frankfurt	PL, SF, K-factor, DS, angle spread
[7]	2.35 GHz	broadband	viaduct scenario in BT HSR	PL, K-factor, Doppler spectrum, DS
[8]	2.35 GHz	broadband	indoor part of train carriage in BT HSR	PL model, K-factor, DS

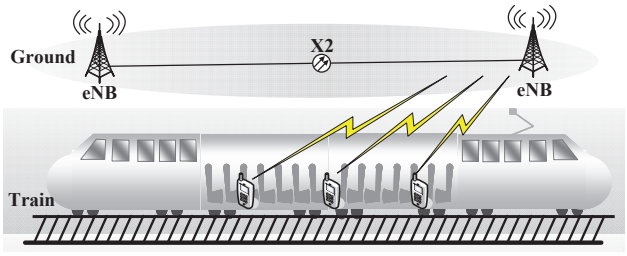

Fig. 1. One-hop network structure of LTE system on HSR

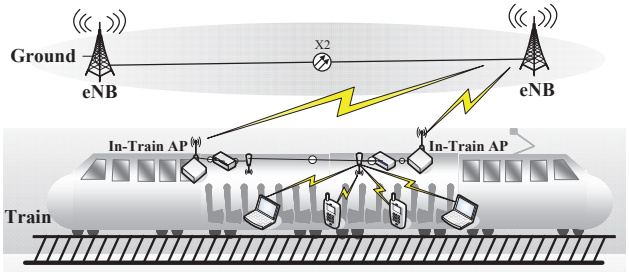

Fig. 2. Two-hop network structure of LTE system on HSR

in HSR scenario, passengers must directly communicate with the base station (BS) near the rails as shown in Fig.1. This one-hop structure is widely used in China for GSM system. The signal encounters reflection, refraction and diffraction both inside and outside the carriage, and especially an about 20 dB penetration loss, resulting in spotty coverage and high drop-call-rate. Secondly, the one-hop structure causes a huge handover burden since dozens of mobile terminals on the train need to be switched simultaneously in the edge of the cell. In addition, to work properly on high speed trains, the mobile station (MS) needs advanced technologies to combat the influence of Doppler shift. It increases the complexity and the cost of terminals. Therefore, the hierarchical two-hop network structure is proposed and widely accepted [9]. It is very likely to be adopted in China. As shown in Fig.2, the connection between the evolved Node B (eNB) and the train is arranged by using an in-train AP mounted on the roof of the carriage. The link from the AP to the interior of the train is arranged by an interior part of the AP with the antennas mounted on the ceiling of the carriage. In this way, signal penetration loss can be avoided. Secondly, in this structure, the eNB communicates with the in-train AP instead of hundreds of terminals. So the cost of train-ground radio resource management could be reduced significantly. Taking the mentioned handover into account, dozens of handovers occur simultaneously in one-hop structure, while, with two-hop structure, only one group-handover is needed. It resolves the problem of high drop-call-rate. Additionally, the In-train APs are expected to support various popular standards such as Wi-Fi, GSM, WCDMA and LTE to satisfy all kinds of wireless access requirements by passengers.

III. MEASUREMENT ENVIRONMENT AND THE SYSTEM

A. Measurement environment

The measurements were conducted on Harbin-Dalian (HD) Railway passenger-dedicated line with an overall length of 903.9 km. Over two-thirds of the line is in viaduct environment, with 162 viaduct bridges and a total length of 663 km. So, in this paper, we focus on the viaduct scenario. The results of our measurements in plain scenario have been reported in [10]. By the approval of the Ministry of Railways of China, The train CRH380B with 8 carriages was used exclusively for measurement purposes and the Tx antenna was mounted on the reserve platform of the signal tower also by approval. The height of signal tower was 40 m and it was positioned 20 m away from the track as shown in Fig.3. The test train carried receiving equipments traversed back and forth on a track of 60 km and run through sounding signal-covered area at a speed of 370 km/h. Mounted on the roof-top of the carriage, the height of receive (Rx) antenna height was 3 m above the rail and the height of rail was 5 m. As shown in Fig.3, The measurement scenario was covered with agricultural fields and the fluctuation of the ground is small. In addition, the viaduct raised the antennas and reduced the number of the scatterers, all these created a relatively ”clear” scenario.

B. Measurement system

Our measurement system is based on slippage correlation algorithm. The principle and the equipments have been reported in [11]. The procedures are illustrated in Fig.4. The measurements were conducted at 2.6 GHz with 20 MHz bandwidth by transmitting a periodic PN sequence with a length of 1023. Data generated by an Agilent E4438C VSG was modulated, up-conversed and amplified to 33 dBm. Then it was directly sent into Tx antenna, which was omni-directional and cross-polarized with 18 dBi gain, 65° horizontal and 7° vertical beam width. Received data was gathered and sampled by an Agilent N9030 VSA temporarily from the 3

A B

Fig. 3. Measurement environment. A.Viaduct scenario. B.The Tx antenna

dBi omni-directional Rx antenna, and then raw in-phase (I) and quadrature (Q) data recorded in a PC for offline data processing.

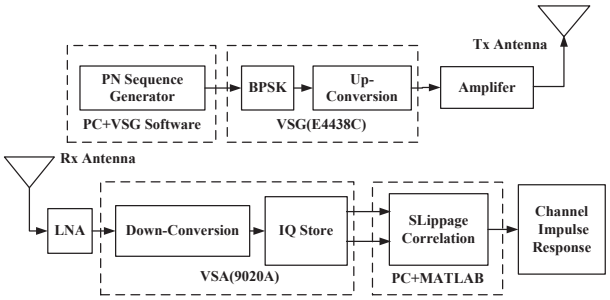

Fig. 4. The block diagram of measurement system

IV. Large-scale fading characteristics analysis and results discussion

Considering the analysis of measured data, large-scale fading describes the slow fluctuation of signal parameters, while small-scale fading predicts the rapid undulation of signal characteristics over a short period of time or distance [9]. So the analysis of data can be divided into these two parts.

A. Path loss exponent

Due to the good autocorrelation property of PN sequence, the CIR is acquired continuously at regular intervals of Tx and Rx separation. For determined point d, $PL(d)$ is the difference of the power at the Tx and Rx

$$PL(d)[dB] = P_{Tx}[dBm] - P_{Rx}(d)[dBm] \qquad (1)$$

where P_{Tx} is 33 dBm as mentioned.

Then gathered CIRs are averaged in squared magnitude and summed over the delay domain to give an average P_{Rx}, in which the influence of small -scale fading has been removed [12].

$$P_{Rx}(it_{av}, k\Delta\tau) = \frac{1}{L}\sum_{n=iL}^{(i+1)L-1}\sum_{k=0}^{K-1} h\left|(nt_{rep}, k\Delta\tau)\right|^2 \qquad (2)$$

where t_{av} and $\Delta\tau$ represent the average time interval and time delay resolution, $h(t,\tau)$ represents the complex CIR at t-th sample instant, t_{rep} is the snapshot repetition period, K is the number of paths and L denotes the number of average snapshots. In this paper, 20 wavelengths are equal to 2.31 m, considering the running speed of 370 km/h, and the averaging time t_{av} is 22.5 ms, thus approximately L=20 snapshots.

The PL model is denoted in (3). In response to a separation d between Tx and Rx in meter, the PL is given by

$$PL(d) = PL(d_0) + 10n\log\left(\frac{d}{d_0}\right) + X_\sigma[dB] \qquad (3)$$

where $PL(d_0)$ is the PL at a reference distance d_0, n is PL exponent and X_σ represents SF.

By fitting the data via linear regression in the minimum mean-square error sense, the PL exponent n is stated concretely in Fig.5, which shows scatter plot of channel PL as a function of log-distance. The measured data are marked by red squares. The estimated PL is labeled with black dotted line and the free space PL is in blue solid line for contrast. Generally, the received power deserves faster drop off as the train traverses further away from the Tx. The estimated PL exponent is 2.8 that is deviated from the typical value 2 for free-space propagation. This kind of deviation is also observed in WIGWAM project [6] and [7]in which the PL exponent were 4.1 and 3.03 respectively. There are two reasons for the extraordinary behavior of the propagation curve. One is that PL exponent highly depends on the special circumstances. In particular, the influence by viaduct bridges and bridge piers cannot be ignored. The other reason is that the antenna mounted very near the roof of the train. The roof affects the antenna radiation pattern and acts as the ground plane. So it is typical that there appears a null in the radiation pattern.

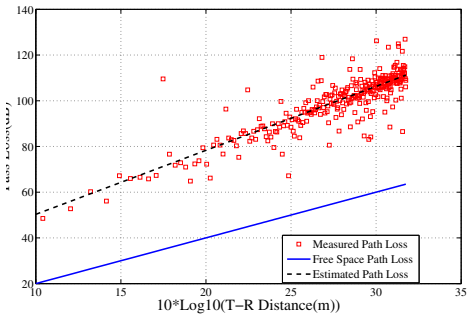

Fig. 5. Measured PL on HD HSR

B. Shadowing fading

Shadowing shows the variation of the actual received power and the overall phenomenon caused by the randomness in the environment. Since, at the distance d, shadowing can be calculated by subtracting the expected PL in model and the realistic measurement results, the equation for PL can be expressed as

$$PL(d) = 22.3 + 28\log(d) + X_\sigma \qquad (4)$$

where X_σ is classically represented by a log-normal distribution with a mean of 0dB and a standard deviation σ=2.49.

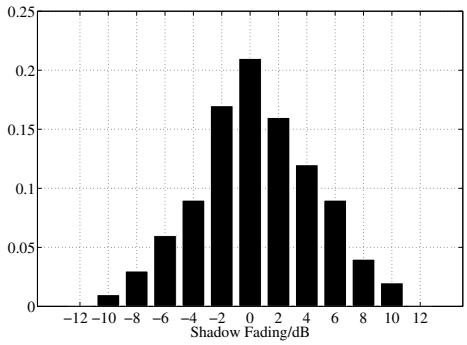

Fig. 6. PDF of SF for HD HSR

Generally, the PDF of the SF as shown in Fig.6. σ=2.49 dB in our measurement and σ=2.0 dB in [7] are relatively small, compared with that in other types of channels [2]. It is mostly due to the fact that measurements are done is "clear" LOS condition and that the train traverses on the high viaduct bridges with few reflection and scattering objects nearby. These parameters and model are useful for link budget and feasible transceiver-range determination of LTE system.

V. Small-scale fading characteristics analysis and results discussion

A. CIR and PDP

The short-time average PDP is calculated by averaging the magnitude squared over 20 wavelengths to remove the influence of small-scale fading. It is represented as

$$P_{PDP}(it_{av}, k\Delta\tau) = \frac{1}{L}\sum_{n=iL}^{(i+1)L-1} h\left|(nt_{rep}, k\Delta\tau)\right|^2 \quad (5)$$

where t_{av} and $\Delta\tau$ represent the average time interval and time delay resolution, $h\left(t,\tau\right)$ represents the complex CIR at t-th sample instant, t_{rep} is the snapshot repetition period and L denotes the number of average snapshots. In this paper, L is 20 snapshots.

Fig.7 demonstrates two typical PDP samples, in which multipath phenomenon, that refers to the paths arriving at the receiver varied widely both in amplitude, phase and time delay can be seen clearly. The values of other paths and the noise are relatively small compared to that of the main path. It is mostly due to the fact that our measurements are done in LOS condition with few scatters and reflectors around.

B. Time delay spread

The DS is one of the key channel characteristics for LTE since it determines the length of cyclic prefix in Orthogonal Frequency Division Multiplexing (OFDM) system.

The RMS delay spread impacts the frequency-selectivity of mobile channel and is commonly used for quantifying DS

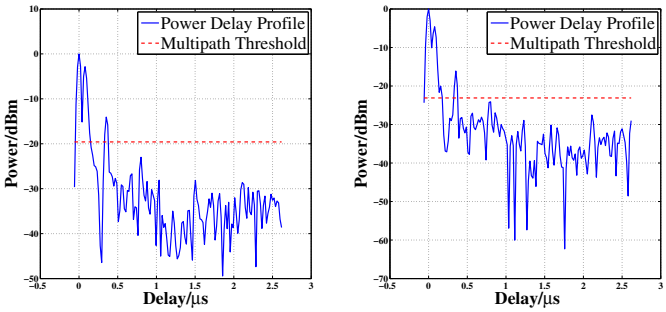

Fig. 7. Typical measured PDPs for HD HSR

characteristics. RMS delay is the square root of the second central moment of the PDP. It is defined as [11]

$$\sigma_\tau = \sqrt{\overline{\tau^2} - (\overline{\tau})^2} \quad (6)$$

where

$$\overline{\tau^2} = \frac{\sum_{k=0}^{K-1}(k\Delta\tau)^2 P_{PDP}(it_{av}, k\Delta\tau)}{\mathrm{P}_{Rx}(it_{av})} \quad (7)$$

and

$$\bar{\tau} = \frac{\sum_{k=0}^{K-1} k\Delta\tau P_{PDP}(it_{av}, k\Delta\tau)}{\mathrm{P}_{Rx}(it_{av})} \quad (8)$$

where t_{av} and $\Delta\tau$ represent the average time interval and time delay resolution, $p\left(t,\tau\right)$ represents the complex PDP at t-th sample instant and K denotes the number of paths.

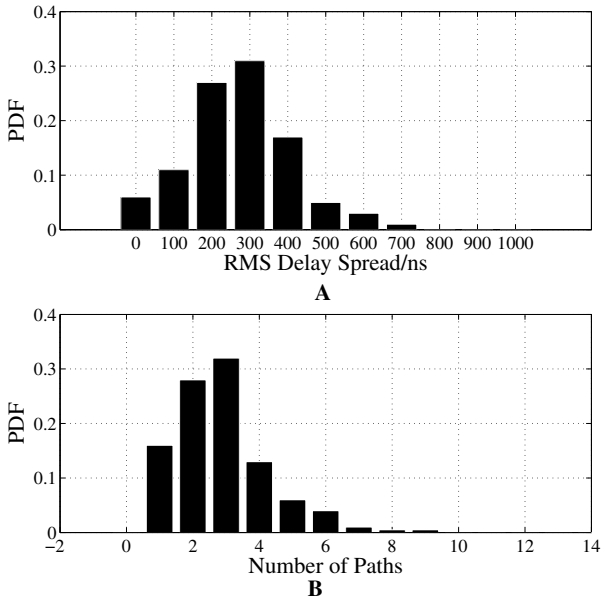

Fig. 8. Basic parameters of DS. A.PDF of RMS DS. B.PDF of the number of paths

Fig.8.A and Fig.8.B depict the PDF of the RMS DS and the number of paths. The value of the RMS delay lies between

0 ns and 700 ns. This time dispersive feature corresponds to frequency selective fading. The highest number of paths depicted in Fig.8.B is 9, and over 90% of the number of paths is between 1 and 5. 3 paths in a measured PDP occurs with the highest probability of 30%.

C. Delay-Doppler spectrum

Due to the remarkable running speed, HSR channel deserves crucial time selectivity that impacts on the average fading rate of the discrete propagation path, which is a challenge to LTE system. The theoretical value of LOS Doppler shift $f_d(t)$ is

$$f_d(t) = \frac{v}{\lambda}\cos(\theta(t)) \tag{9}$$

Where v is the speed of the train and λ represents the wavelength, $\theta(t)$ is the varying angle of the receiving electromagnetic wave and the direction of motion.

The continuous CIR is directly transformed into the Doppler frequency domain by the fast-Fourier transformation (FFT). It is defined as [11]

$$P_{Doppler}(r\Delta v, k\Delta\tau) = f_{fft}\left[h\left(nt_{rep}, k\Delta\tau\right)\right] \tag{10}$$

The width of spread in Fig.9 is called the Doppler spread $f_{\max}$, which is related to the speed and the center frequency. In HD HSR, the speed of 370 km/h leads to a 900 Hz maximum Doppler frequency and the Doppler frequency shift sweeps from a positive value to a negative value with the variation of angle between the incoming wave and the direction of motion.

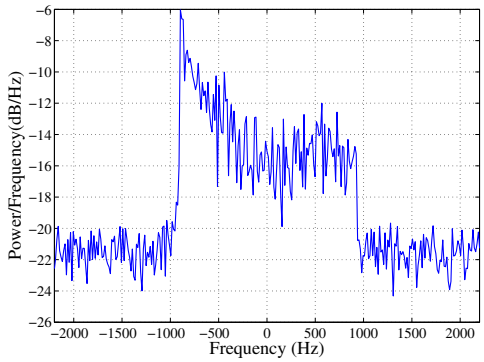

Fig. 9. Doppler spectrum for HD HSR

VI. Conclusion

By the approval of the Ministry of Railways of China, broadband channel measurements at 2.6 GHz for train-ground communications on HSR are first carried out. Using slippage correlation algorithm, extensive and practical measurement campaigns are conducted on HD HSR line under the hierarchical two-hop network structure.

Based on the measured data, a novel path loss model was proposed to predict large-scale signal coverage for viaduct scenarios. The PL exponent n=2.8 deviates from the one in free space condition due to not only the influence by viaduct bridges and bridge piers, but also the affect by the roof of the carriage on antenna radiation pattern. Since the viaduct raises the antennas and reduces the number of the scatterers, it creates a relatively "clear" LOS environment. The shadowing factor with a standard deviation 2.0 shows this small variation. From the delay statistics, the results clearly shows that the RMS delay does not exceed 700 ns and RMS delays of 300 ns occur most frequently. The highest number of paths is 9, and over 90% of the number of paths is between 1 and 5. The Doppler frequency shift sweeps from positive to negative with the variation of the angle between the arriving wave and the direction of motion. The maximum value of Doppler frequency shift is about 900 Hz, which is in accordance with the theoretical derivation results.

The path loss model and derived channel characteristics give a comprehensive and informative description of the radio environments in HSR. These results significantly promote the design and evaluation of LTE system in HSR scenario.

VII. Acknowledgment

This work was supported by the National Science and Technology Major Projects of China under Grant No. 2011ZX03001-007-03.

References

[1] R.He, Z.Zhong, B.Ai, G.Wang, J.Ding, A.Molisch, "Measurements and Analysis of Propagation Channels in High-Speed Railway Viaducts," *IEEE Transactions on Wireless Communications*, vol.12, no.2, pp.794, 805, Feb. 2013.

[2] R.He, Z.Zhong, B.Ai, G.Wang, J.Ding, "Propagation measurements and analysis for high-speed railway cutting scenario," *Electronics Letters*, vol.47, no.21, pp.1167-1168, Oct. 2011.

[3] D.J.Cichon, T.Zwick, W.Wiesbeck, "Ray optical modeling of wireless communications in high-speed railway tunnels," *Vehicular Technology Conference, 1996*, pp.546,550, vol.1, May 1996.

[4] Yinghong Wen, Yunshuang Ma, Xiaoyan Zhang, Xiaojun Jin, Fenglan Wang, "Channel fading statistics in high-speed mobile environment," *Antennas and Propagation in Wireless Communications (APWC)*, pp.1209-1212, 2-7, Sept. 2012.

[5] Jiahui Qiu, Cheng Tao, Liu Liu, Zhenhui Tan, "Broadband Channel Measurement for the High-Speed Railway Based on WCDMA," *Vehicular Technology Conference (VTC Spring)*, pp.1-5, 6-9, May 2012.

[6] K. Pekka, "WINNER II Channel Models part II Radio Channel Measurement and Analysis Results," 2007.

[7] Liu Liu, Cheng Tao, Jiahui Qiu, Houjin Chen, Li Yu, Weihui Dong, Yao Yuan , "Position-Based Modeling for Wireless Channel on High-Speed Railway under a Viaduct at 2.35 GHz", *IEEE Journal on Selected Areas in Communications*, vol.30, no.4, pp.834-845, May 2012.

[8] W. Dong, G. Liu, L. Yu, H. Ding, and J. Zhang, "Channel Properties of indoor part for high-speed train based on wideband channel measurement," in *Proc. 5th Int Communications and Networking in China(CHINACOM) ICST Conf*, Aug. 2010, pp. 1-4.

[9] C.Tao, L.Liu, J.Qiu, and Z.Tan, "Architecture and Key Techniques of Broadband Wireless Access System for High Speed Railway," *Telecommunications Science*, vol.33, no.5, pp.95-101, 2010.

[10] Zhao Min, Wu Muqing, Sun yanzhi, Yu deshui, "Analysis and Modeling for Train-Ground Wireless Wideband Channel of LTE on High-Speed Railway" *Vehicular Technology Conference (VTC Spring)*, 2013.

[11] Zhao Min, Wu Muqing, Guo Song Hu Qian, "Wideband channel measurement at 2.6 GHz using slippage correlation and amplitude distortion correction algorithm", *Advances in Information Sciences and Service Sciences*, pp. 387-394, Oct. 2012.

[12] A. Paier, J. Karedal, N. Czink, H. Hofstetter, C. Dumard, T. Zemen, F. Tufvesson, C.F. Mecklenbrauker, A.F. Molisch, "First Results from Car-to-Car and Car-to-Infrastructure Radio Channel Measurements at 5.2GHZ," *Personal Indoor and Mobile Radio Communications, PIMRC 2007. IEEE 18th International Symposium*, pp.1-5, 3-7 Sept. 2007.